doi:10.1093/plphys/kiaa032 PLANT PHYSIOLOGY 2021: 185: 503–518

Plant Physiology

Research Article

Characterization of *CYCLOPHILLIN38* shows that a photosynthesis-derived systemic signal controls lateral root emergence

Lina Duan [1,2] Juan Manuel Pérez-Ruiz [3] Francisco Javier Cejudo [3] and José R. Dinneny [1,2,*,†]

1 Biology Department, Stanford University, Stanford, CA 94305, USA
2 Department of Plant Biology, Carnegie Institution for Science, Stanford, CA 94305, USA
3 Instituto de Bioquímica Vegetal y Fotosíntesis, Universidad de Sevilla and Consejo Superior de Investigaciones Científicas, Avda Américo Vespucio 49, 41092 Sevilla, Spain

*Author for communication: dinneny@stanford.edu
†Senior author.

L.D., J.M.P., F.J.C., and J.R.D. designed this study. L.D. performed the mutant screen, phenotypic analysis, cloning, imaging, and performed the data analysis. J.M.P. performed the biochemistry studies and measurements of photosynthesis parameters. L.D., J.M.P, F.J.C., and J.R.D. wrote and revised the manuscript.
The author responsible for distribution of materials integral to the findings presented in this article in accordance with the policy described in the Instructions for Authors (https://academic.oup.com/plphys) is: José R. Dinneny (dinneny@stanford.edu).

Abstract

Photosynthesis in leaves generates fixed-carbon resources and essential metabolites that support sink tissues, such as roots. Two of these metabolites, sucrose and auxin, promote growth in root systems, but the explicit connection between photosynthetic activity and control of root architecture has not been explored. Through a mutant screen to identify pathways regulating root system architecture, we identified a mutation in the *Arabidopsis thaliana CYCLOPHILIN 38* (*CYP38*) gene, which causes accumulation of pre-emergent stage lateral roots. *CYP38* was previously reported to stabilize photosystem II (PSII) in chloroplasts. *CYP38* expression is enriched in shoots, and grafting experiments show that the gene acts non-cell-autonomously to promote lateral root emergence. Growth of wild-type plants under low-light conditions phenocopies the *cyp38* lateral root emergence defect, as does the inhibition of PSII-dependent electron transport or Nicotinamide adenine dinucleotide phosphate (NADPH) production. Importantly, these perturbations to photosynthetic activity rapidly suppress lateral root emergence, which is separate from their effects on shoot size. Supplementary exogenous sucrose largely rescued primary root (PR) growth in *cyp38*, but not lateral root growth. Auxin (indole-3-acetic acid (IAA)) biosynthesis from tryptophan is dependent on reductant generated during photosynthesis. Consistently, we found that wild-type seedlings grown under low light and *cyp38* mutants have highly diminished levels of IAA in root tissues. IAA treatment rescued the *cyp38* lateral root defect, revealing that photosynthesis promotes lateral root emergence partly through IAA biosynthesis. These data directly confirm the importance of CYP38-dependent photosynthetic activity in supporting root growth, and define the specific contributions of two metabolites in refining root architecture under light-limited conditions.

Introduction

The coordination of shoot and root system growth is highly dependent on environmental context (Bloom, 2005; Puig et al., 2012). Previous research has shown that the limitation of water or nutrients in soil can enhance the growth of the root system relative to the shoot (Rellán-Álvarez et al., 2015). Conversely, shoot tissues can also have a positive effect on root system branching (Wightman and Thimann,

Received August 18, 2020. Accepted October 29, 2020. Advance access publication November 27, 2020

1980; Bhalerao et al., 2002). Initial studies investigating the role of shoot-derived signals in promoting root growth demonstrated that the excision of tissues from the seedling shoot inhibited the emergence of lateral root (LR) primordia. The critical signal transmitted from shoot to root was later identified as auxin (McDavid et al., 1972; Rost, 1986). Using radiotracing to track transport, auxin applied to shoot tissues was later detected in roots (Rowntree and Morris, 1979; Kerk and Feldman, 1995; Reed et al., 1998). Furthermore, localized application of an auxin-transport inhibitor to the root/shoot junction prevented the transport of labeled auxin to roots and inhibited LR emergence. Later studies used transgenes to express orthogonal auxin-biosynthetic enzymes in shoot tissues and showed that auxin biosynthesis in the shoot is sufficient to promote LR emergence (Swarup et al., 2008). It has been suggested that the initiation of LRs is promoted by root tip-derived auxin, while emergence is promoted from the shoot (Laskowski et al., 1995; Bhalerao et al., 2002).

The signaling pathways controlling the synthesis and transport of auxin from the shoot to root are currently being explored, but light intensity appears to be a critical component (Halliday et al., 2009). Hersch et al. showed that auxin levels increased as a consequence of increased irradiance of seedlings with light; however, light quality, manipulated by changing the ratio of red to far-red light, also influences auxin accumulation (Hersch et al., 2014). Bhalero et al. showed that LR emergence, and the associated shoot-derived auxin pulse that occurs after germination, is dependent on seedling exposure to light (Bhalerao et al., 2002). While light was shown to be necessary for shoot-mediated auxin accumulation in roots, whether this is dependent on photosynthetic activity or other light-signaling pathways has not been determined. Light perception by wavelength-specific photoreceptors regulates the production of auxin in the shoot to affect hypocotyl elongation (de Wit et al., 2016). Auxin-independent mechanisms for light-regulated root growth also exist. ELONGATED HYPOCOTYL 5 (HY5) protein accumulates in a light-dependent manner, downstream of photoreceptor signaling, and translocates to the root to promote root branching (Chen et al., 2016; Van Gelderen et al., 2018; Zhang et al., 2019). Nevertheless, the relationship between these various light-sensitive pathways is still unclear, as is the potential role of photoreceptor-independent mechanisms in the systemic control of root architecture.

From a resource-centric point of view, the plant body can be separated into two domains: source tissues, which generate resources, and sink tissues, which use these resources (Chang et al., 2017). Root system growth predominantly occurs below ground in most species, and requires the products of photosynthesis from shoots (Bloom, 2005). Sucrose is an important transport molecule that provides the energy for metabolism and the carbon-based building blocks for growth. Previous work has demonstrated that PR growth is limited in seedlings grown in the dark, while supplementing with exogenous sucrose can rescue this effect (Kircher and Schopfer, 2012). Photosynthesis also generates the reductant NADPH, which is used in the biosynthesis of a number of metabolites. In particular, the conversion of indole-3-pyruvate acid (IPA) to indole-3-acetic acid (IAA), the natural form of auxin, utilizes the redox power of NADPH in the reaction (Mashiguchi et al., 2011; Zhao, 2012). What role these products of photosynthesis play in light-regulated LR growth has not been explored, which limits our ability to determine the relative contributions of photosynthesis-dependent metabolite production and photoreceptor-dependent signaling to root system architecture.

LR emergence is a complex developmental process that integrates both new organ morphogenesis and structural change of the old root tissue. LRs form through oriented cell divisions within the pericycle tissue layer, which is hidden three layers deep inside the parent root (Van Norman et al., 2013). The positioning of LRs along the pericycle cell profile and the formation of LR founder cells are determined by the oscillation of auxin signaling (Moreno-Risueno et al., 2010). A dome-shaped lateral root primordia (LRP) is then formed after a series of cell divisions. The penetration of LRP through the outer tissues of the parent root requires auxin transport and signaling to change the mechanical properties of the three overlying tissue layers (Swarup et al., 2008; Lucas et al., 2013; Vermeer et al., 2014).

In this study, we specifically explore the role that photosynthesis plays in the systemic regulation of LR emergence by shoots. We identified a mutant that strongly inhibits LR emergence and revealed that the causative mutation disrupts *CYCLOPHILIN 38* gene function, which normally promotes the assembly of photosystem II (PSII; Fu et al., 2007). The effects of the *cyp38* mutation on root architecture are systemic, shoot-specific, and mimicked by the growth of seedlings with reduced light irradiance or inhibitors of light-dependent electron transport. We reveal that the *cyp38* mutation or low light intensity causes a dramatic reduction in auxin biosynthesis, and the effect of these perturbations on LR emergence can be rescued with exogenous auxin treatment. Finally, genetic analysis of *hy5* mutants reveals that this photoreceptor-dependent pathway likely acts in parallel to the photosynthesis-dependent pathway defined here, thus revealing multiple levels of regulation that coordinate root growth with shoot physiology.

Results

CYP38 is necessary for LR emergence

To identify factors that play a role in LR emergence, we conducted a mutant screen and characterized a recessive mutant (originally named *prematurely stunted lateral organs, presto*) that exhibits a severe reduction (85.4% reduction) in LR density under standard growth conditions, compared to wild-type (WT), while PR growth is also significantly reduced, but to a lesser extent (51% reduction; Figure 1, A–C). Next-generation ethyl methanesulfonate (EMS) mutation mapping using sequencing was used to identify the causative genetic locus, *CYCLOPHILIN 38* (*CYP38;* Supplemental Figure S1). A T-DNA allele (*cyp38-5*) with an insertion in the sixth exon phenocopied the EMS allele (*cyp38-4;* Figure 1,

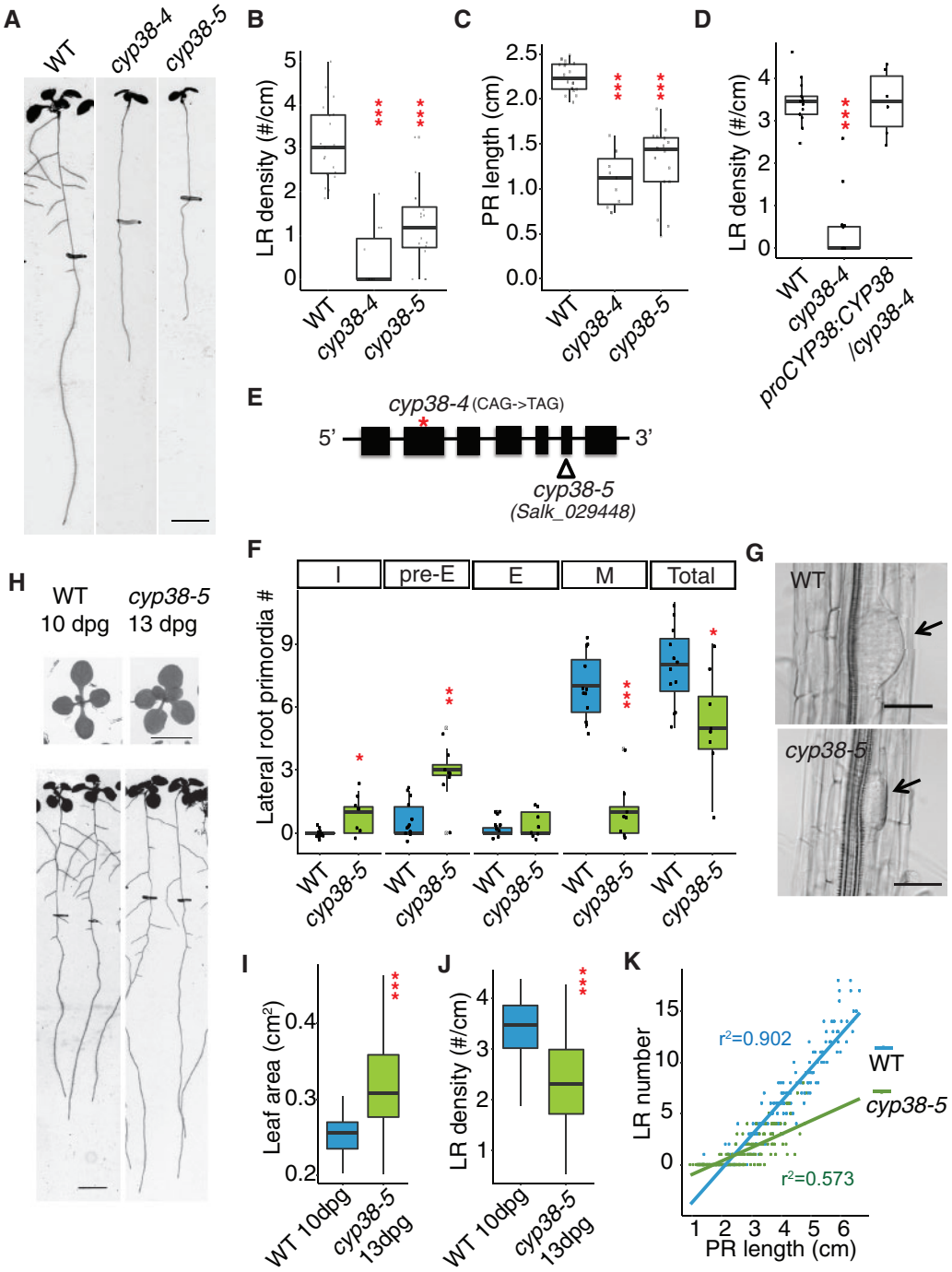

Figure 1 *CYP38* is required for LR emergence. **A**, Scanned root images of 11-dpg WT, *cyp38-4* and *cyp38-5*. 6-dpg root tip positions are labeled with black marks. Scale bar = 5 mm. **B** and **C**, Quantifications of LR density (**B**) and PR length (**C**) in two alleles of *cyp38*. (***$P < 0.001$, pairwise *t* test with Hochberg correction, $n > 10$). **D**, Quantifications of LR density of the EMS allele, *cyp38-4*, and the complemented line. (***$P < 0.001$, pairwise *t* test with Hochberg correction, six complemented T1 plants are used). **E**, Diagram describing the mutation position of *cyp38-4* (red asterisk) and T-DNA insertion position of *cyp38-5* (triangle). **F**, Quantifications of different stages of LRP in WT and *cyp38-5*. I represents the initiation stage, pre-E represents pre-emergence stage, E represents emerged LR stage, M represents matured LRs, and Total represents the sum of all four stages. (*$P < 0.05$, ***$P < 0.01$, ***$P < 0.001$, pairwise *t* test with Hochberg correction, $n > 8$). **G**, Microscopic images of cleared WT and *cyp38-5* roots. Arrows point to pre-emerged LRP. Scale bar = 50 μm. **H**, Scanned shoot and root images of 10-dpg WT and 13-dpg *cyp38-5*. Root tip positions of 6-dpg are labeled with black marks. Scale bars = 5 mm. **I** and **J**, Quantifications of shoot area (**I**) and LR density (**J**) in 10-dpg WT and 13-dpg *cyp38-5*. (***$P < 0.001$, pairwise *t* test, $n > 20$). **K**, Quantifications of LR number over PR length were made with 6- to 10-d-old WT and *cyp38-5* roots. Data points obtained at each day are pooled to generate scatter plot. Linear regression lines are added to show their trend.

A–C), which has an early stop codon in the second exon (Figure 1E; Supplemental Figure S1). Expression of *CYP38* using its native promoter fully complemented *cyp38-4* (Figure 1D), indicating that *CYP38* is indeed the causative gene.

To determine the developmental basis for the *cyp38* phenotype, we classified LR growth into four distinct stages (Malamy and Benfey, 1997; Duan et al., 2013; Orman-Ligeza et al., 2016): initiation (I, including stages I–III), pre-emergence (Pre-E, including stages IV–VII), emergence (E), and mature LR (M; Supplemental Figure S1B). Compared to WT, where the majority of LRs have typically progressed to the maturation stage in 8-d post germination (dpg) seedlings, we found that *cyp38-5* mutants had a significant enrichment of pre-emergence stage LRs (Figure 1F). LRP exhibited a flattened shape in *cyp38-5* instead of the typical dome shape observed in WT (Figure 1G). This defect has also been observed in other mutants that specifically affect the emergence stage (Péret et al., 2012; Fernández-Marcos et al., 2017). It is likely that initiation and/or founder cell specification stages may also be disrupted to account for the full reduction in LR development.

Previous work studying the effects of mutations in *CYP38* demonstrated that shoot growth is reduced, particularly under high-light intensity growing conditions (Fu et al., 2007). Since the amount of shoot tissues corresponds with root growth, this raises the possibility that the observed changes in LR development in *cyp38* are merely an indirect effect of the overall slower growth of the seedling rather than a direct effect of changes in the photosynthetic activity. Indeed, the total number of LRs (pre- and post-emergence) per seedling was reduced in *cyp38* mutants, compared to WT, consistent with an overall slower rate of seedling development (Figure 1F). However, a closer examination of the LR growth defect revealed that development was not uniformly affected. For example, the number of pre-emergence stage LRs showed a trend opposite of what we expected, with an increase relative to WT. Further evidence that shoot size differences do not fully explain the changes in LR development come from comparisons between seedlings of different ages. In 13-dpg *cyp38-5* seedlings, shoot size was measured to be 23.9% larger than WT, while LR emergence was still 32% reduced relative to WT at 10 dpg (Figure 1, H–J). We also analyzed the allometric relationship between PR length and LR number in a 5-d time course (roots were imaged every 24 h from 6 to 10 dpg). Plotting of these data show that WT PR length shows a linear relationship with LR number and that this correlation is less positive for *cyp38* (r^2 = 0.902, WT; 0.573, *cyp38-5*; Figure 1K). These differences are inconsistent with the hypothesis that the *cyp38* growth is simply delayed as one would expect allometric relationships to be maintained. Together these data strongly suggest that the developmental program of *cyp38* is altered substantially and specifically, leading to a change in root architecture as a consequence of defects in LR emergence, and that these defects are not fully explained by the reduction in shoot size.

CYP38 is primarily localized to the chloroplast

As previously reported, *CYP38* encodes a cyclophilin-related protein important in the assembly and stability of PSII under high light (Fu et al., 2007; Sirpiö et al., 2008; Vasudevan et al., 2012). However, limited characterization of the tissue-specific and subcellular localization of the protein has been performed. A transcriptional fusion, *proCYP38::erGFP*, and quantitative Reverse Transcription Polymerase Chain Reaction (RT-PCR) indicated that the gene is expressed predominantly in shoot tissues (mesophyll and hypocotyl; Figure 2, A and B). While we observed low levels of reporter expression in root regions that are close to the hypocotyl, very little fluorescence could be detected in LRP and root tips (Figure 2A). Transient expression of a Ypet-tagged translational fusion to *CYP38* in Arabidopsis protoplasts showed a chloroplast-specific localization pattern (Figure 2C). In stably transformed plants, only chloroplast localization was observed (Figure 2D). These data are consistent with a chloroplast-specific function for CYP38 in Arabidopsis.

CYP38 regulates LR emergence through systemic signals

We next used grafting to resolve whether *CYP38* function in the shoot or root is responsible for the LR growth defects observed. Both WT and *cyp38-5* mutant scions were grafted to WT or *cyp38-5* root stocks. Root branching was quantified 12-d post-grafting. Because we observed senescence of the PR tip after formation of the graft junction, we quantified the total number of branches formed instead of LR density. Interestingly, grafting of a WT scion onto a *cyp38-5* root stock significantly rescued the LR emergence defect while a *cyp38-5* scion caused the WT root stock to exhibit a *cyp38*-like phenotype (Figure 3, A and B). These data suggest that the LR emergence phenotype is determined primarily by the genotype of the shoot.

As previously reported in tomato, the CYCLOPHILIN protein DIAGETROPICA promotes root branching by moving from the shoot to root (Ivanchenko et al., 2015; Spiegelman et al., 2015). To investigate whether *CYP38* mRNA or protein is able to translocate across the shoot–root junction, we compared expression in shoot and root tissues of the four grafted combinations described above. Interestingly, the *CYP38* transcript remained low in the WT/*cyp38-5* rootstock despite the LR development being rescued. The transcript level in *cyp38-5*/WT scion is increased relative to the *cyp38-5* mutant root system; however, the levels are very low compared with the WT shoot (Figure 3C). Thus, we conclude that there is little to no movement of *CYP38* mRNA across the shoot–root junction. Similarly, we also examined protein movement by grafting the shoot of *proUBQ10:CYP38-Ypet/cyp38-5* transgenic lines with a *cyp38-5* mutant root or shoot. Confocal microscopy was used to detect yellow fluorescence at the shoot–root junction after the graft junction formed successfully (about 5- to 7-d post-grafting). No substantial fluorescence could be detected across the grafted junction (Figure 3, D and E). Grafting of *proUBQ10:CYP38-Ypet/cyp38-5* onto *cyp38* mutant root stocks resulted in a

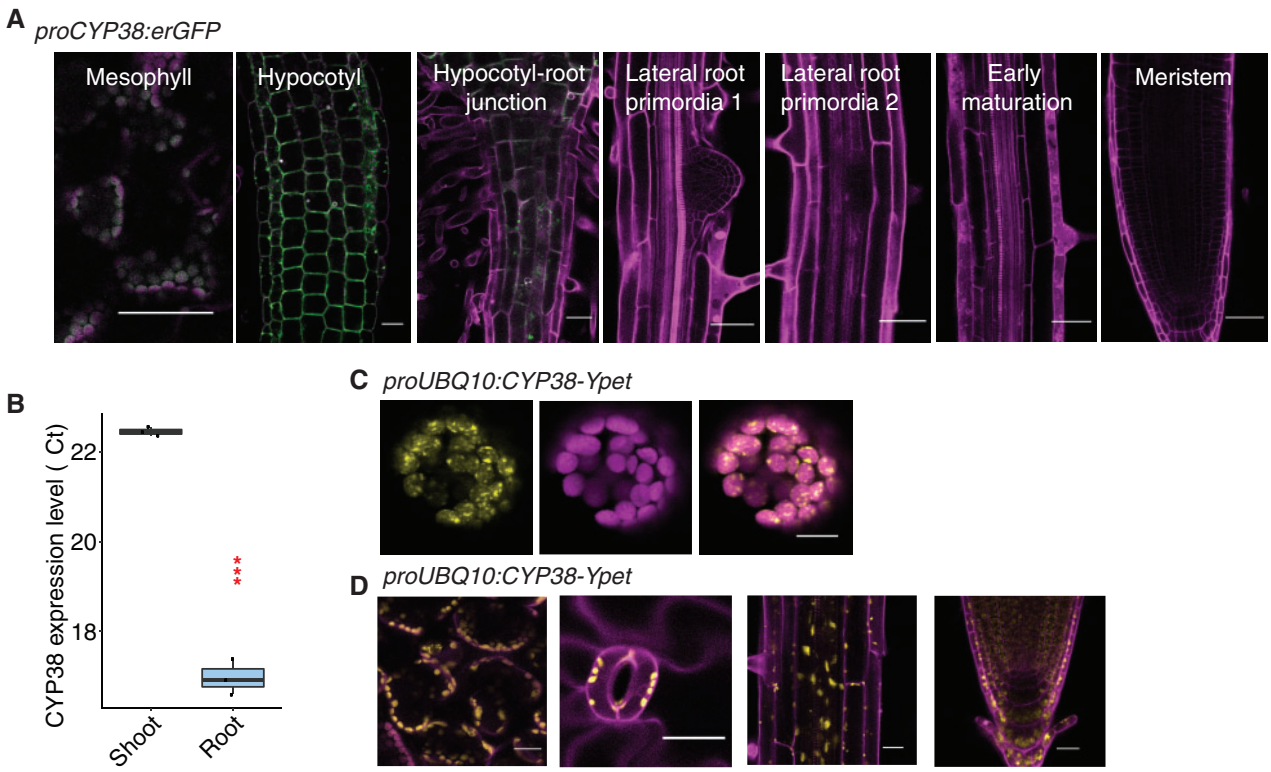

Figure 2 CYP38 is highly expressed in shoots and localized in plastids. **A**, Confocal images of *proCYP38:erGFP* transgenic line. Magenta indicates autofluorescence of chloroplasts in mesophyll cells together with PI staining in the hypocotyl and various regions of the root, while green indicates GFP fluorescence. Scale bars = 50 μm. **B**, Quantitative RT-PCR of *CYP38* transcript level in WT shoot and root tissue. The numbers are presented as $\log_2$ transformed values ($\Delta\Delta C_t$). (***$P < 0.001$, pairwise *t* test, $n = 3$). **C**, Confocal images of WT protoplast that was transiently transformed with *proUBQ10:CYP38-Ypet*. Magenta indicates chloroplast autofluorescence, while yellow indicates Ypet fluorescence. Scale bars = 10 μm. **D**, Confocal images of *proUBQ10:CYP38-Ypet* transgene fluorescence in various tissues including (left to right) mesophyll, stomata, mature root and root tip. Magenta indicates PI staining and autofluorescence from chloroplasts while yellow indicates Ypet fluorescence. Scale bars = 20 μm.

rescue of LR emergence, indicating the fusion protein was functional (Supplemental Figure S2). In summary, the chloroplast localization pattern of CYP38 is consistent with previous findings on the importance of CYP38 in photosystem stability. The limited mobility of both mRNA and protein indicates that CYP38 promotes LR emergence non-autonomously from photosynthetic shoot tissues.

Reduced quantity of light suppresses LR emergence

To determine whether the defect in LR emergence in *cyp38* mutants is a result of changes in overall photosynthetic activity, we first examined what effect light intensity had on root architecture. Importantly, while previous studies have demonstrated that treatment of seedlings with darkness inhibits LR emergence, this extreme change in light intensity may have many indirect effects on physiology. We manipulated light intensities by layering sheets of window screen to block varying amounts of light, which we found reduces the intensity of the light without affecting the spectrum, particularly the red/far red light ratio (Supplemental Figure S3, A and B). Arabidopsis seedlings were grown under standard light conditions (~140 μE m^{-2} s^{-1}) for 5 d and then transferred to several reduced light intensities and grown for an additional 4 d. A severe reduction in emerged LRs (up to 92% reduction) and total LR length (up to 96.6% reduction) was observed when light intensity declined (Figure 4, A and B and Supplemental Figure S3C), while PR growth was moderately affected (up to 32% reduction; Figure 4, A and C). Intriguingly, light intensity affected LR emergence rapidly in seedlings transferred from standard to low light conditions; after 1 d of low-light treatment we observed a significant reduction in the number of emerged LRs (Figure 4, D and E). We found that as the light intensity declined, LRs were increasingly enriched at the pre-emergence stage (Figure 4F), indicating that this response reflected a specific inhibitory effect on the process of LR emergence rather than a general reduction in growth. LR development is not necessarily always most restricted when seedling growth is inhibited, as our previous study showed that treatment with 1-aminocyclopropane-1-carboxylic acid inhibited PR growth more effectively than LRs (Duan et al., 2013).

To investigate whether the specific developmental response to light intensity is due to the direct perception of light by the root system in our tissue culture conditions, we utilized the Growth and Luminescence Observatory for Roots system to recapitulate a more physiologically relevant condition where roots are shielded from light and grown in soil (Rellán-Álvarez et al., 2015). Using this system, we

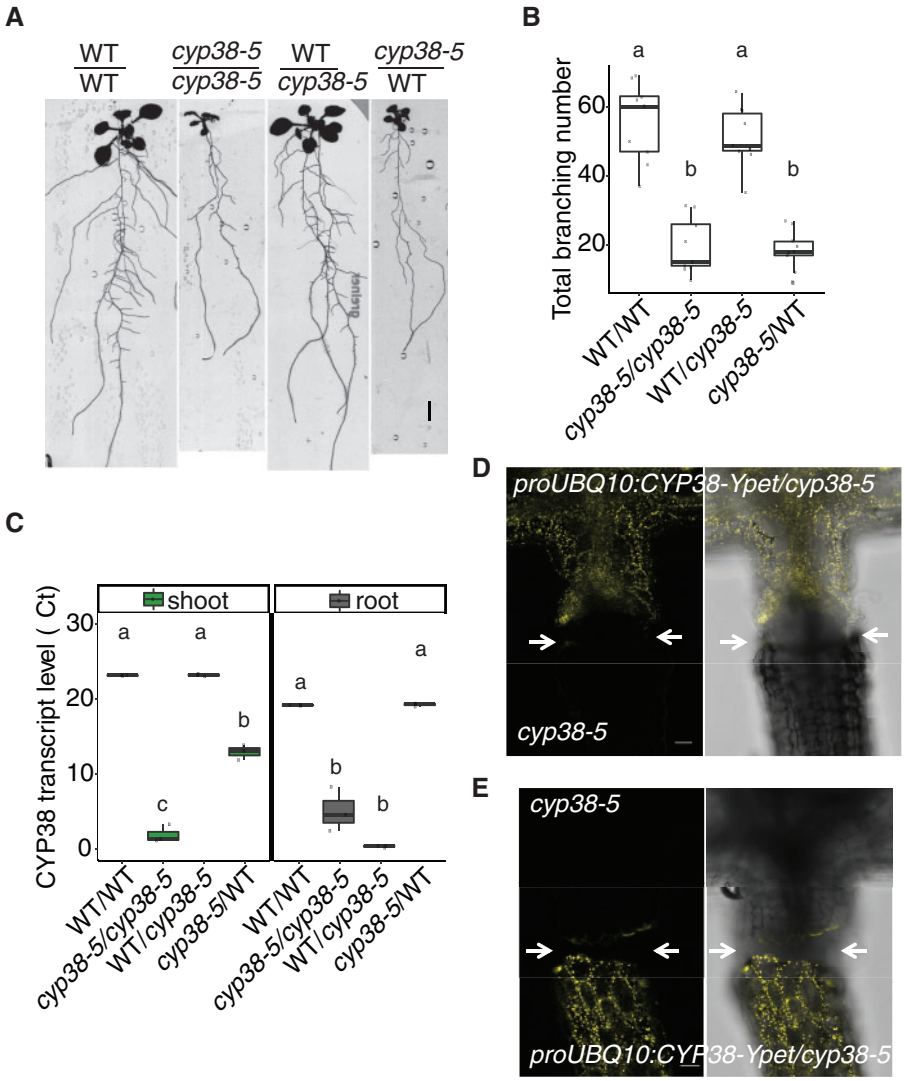

Figure 3 The activity of CYP38 in shoots is essential for LR emergence. **A**, Scanned root images of 17-d-old grafted plants. Seedlings were grafted 5 dpg, graft junction was formed after 5 d on filter paper and then the whole grafted plants were transferred back to regular medium for 7 d to recover. Scale bar = 5 mm. **B**, Quantification of total branch number in four different grafted combinations. Significantly different groups are indicated with letters ($P < 0.05$, pairwise *t* test with Hochberg correction, $n > 8$). **C**, Quantitative RT-PCR for *CYP38* transcript levels in both shoot and root tissues of the grafted plants. The numbers are presented as $\log_2$ transformed values ($\Delta\Delta C_t$). Significantly different groups are denoted with letters ($P < 0.05$, pairwise *t* test with Hochberg correction, $n = 3$) and analyzed separately for shoot and root samples. **D** and **E**, Confocal images of the hypocotyl junction in grafted plants. *proUBQ10:CYP38-Ypet* is used as the scion in (**D**), or used as the rootstock in (**E**). Arrows mark the grafting junction. Scale bars = 50 μm.

observed a significant reduction in the number of LRs in *cyp38-5* mutant plants compared to WT; a similar effect was observed in plants grown under low-light conditions (Supplemental Figure S3, D and E). These data indicate that in both tissue culture conditions and soil conditions, the amount of light perceived by the shoot has a specific promoting effect on LR development that is distinguishable from the overall effect on growth.

Photosystem stability and chloroplast redox state regulate LR emergence

To directly test whether the activity of the photosynthetic apparatus is required for LR emergence, we treated seedlings with 3-(3,4-dichlorophenyl)-1,1-dimethylurea (DCMU), which is a well-characterized inhibitor of electron transport between PSII and PSI. While we observed a nearly complete block of LR emergence with 2 μM DCMU, 1 μM DCMU caused a less severe reduction (41.5% reduction; Figure 5, A and B). Consistent with other experiments affecting the photosynthetic activity, PR growth was affected to a lesser extent than LRs (18.2% reduction; Figure 5A; Supplemental Figure S4A).

We hypothesized that the products of the electron transport chain, such as NADPH or other downstream reducing agents may play important roles in modulating LR development. Consistent with this hypothesis, a reduction in LR

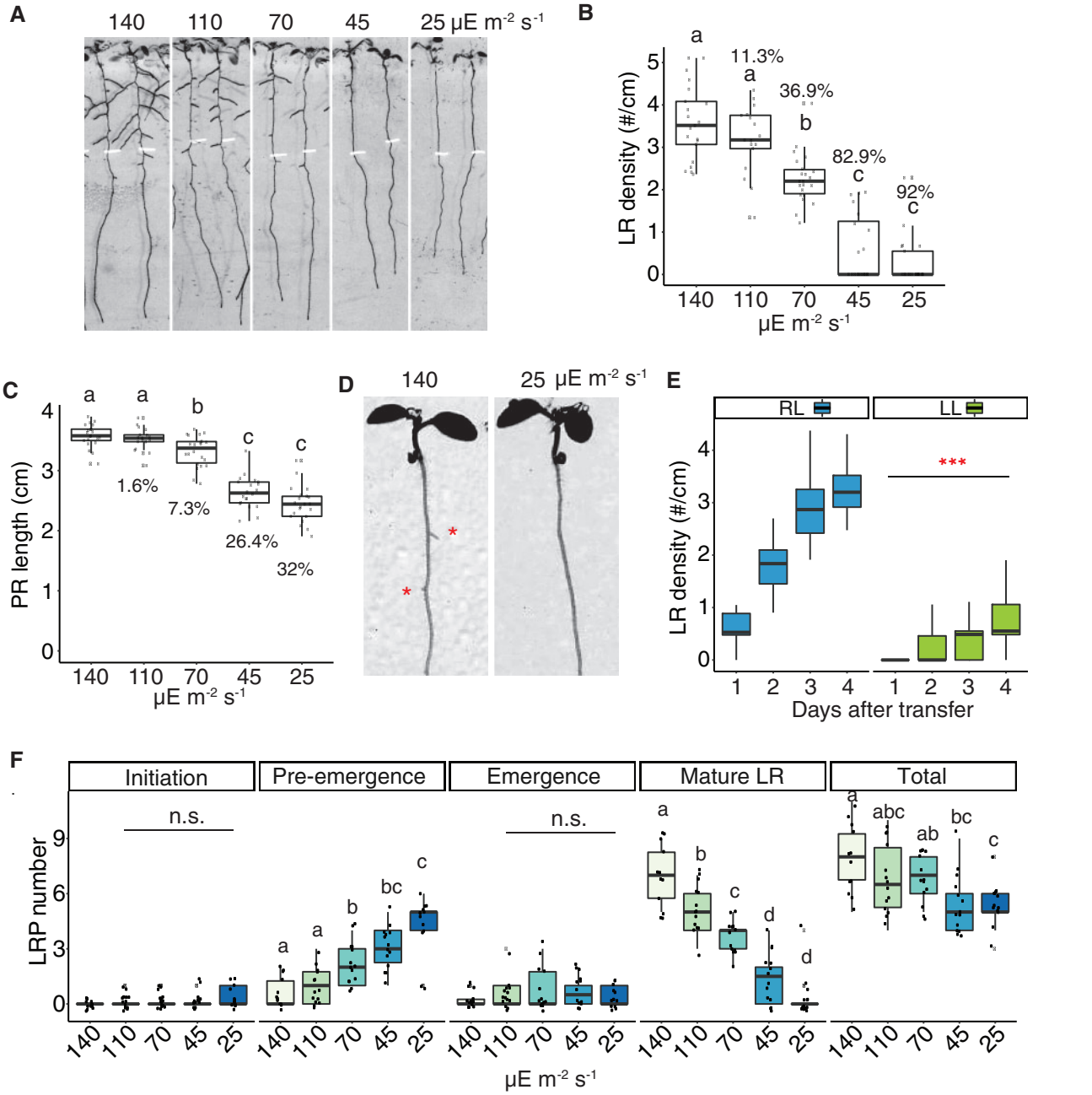

Figure 4 Reducing light quantity inhibits LR emergence. **A**, Scanned root image of 9-dpg WT seedlings grown under 140-μE light for 5 d and then transferred to different light intensities for another 4 d. Root tip positions of 5-dpg are labeled with white marks. **B** and **C**, Quantification of LR density (**B**) and PR length (**C**) in WT under different light intensities. Percentage reduction compared with control light condition (140 μE m^{-2} s^{-1}) is labeled on each box. Significantly different groups are indicated with letters ($P < 0.05$, pairwise *t* test with Hochberg correction, $n > 16$). **D**, Scanned root images. WT was grown under standard light for 6 d and then transferred to low light for 1 d. Red asterisks mark the emerged LRP. **E**, Quantification of LR density in WT after 1–4 d treatment of regular (RL) or low light (LL). (***$P < 0.001$, pairwise *t* test, $n > 25$). **F**, Quantification of different stages of LRP in WT under different light intensities. Total represents the sum of all previous four stages. Significantly different groups are indicated with letters ($P < 0.05$, pairwise *t* test with Hochberg correction, $n > 12$).

growth was reported in mutant plants devoid of NADPH-dependent thioredoxin (Trx) reductase C (NTRC; Kirchsteiger et al., 2012), a chloroplast enzyme (Serrato et al., 2004) that plays a central role in redox regulation of chloroplast proteins. NTRC is the most efficient electron donor to 2-Cys peroxiredoxins (Prxs), thereby the NTRC-2-Cys Prx redox system maintains the reductive capacity of chloroplast Trxs, allowing the proper regulation of their targets (Pérez-Ruiz et al., 2017). To further characterize the contribution to LR development of these redox systems, NTRC-2-Cys Prx and Trxs, we evaluated the various mutants reported, which experience impaired redox homeostasis to different extents (Pérez-Ruiz et al., 2017). Interestingly, although only mild reduction in LR emergence was observed

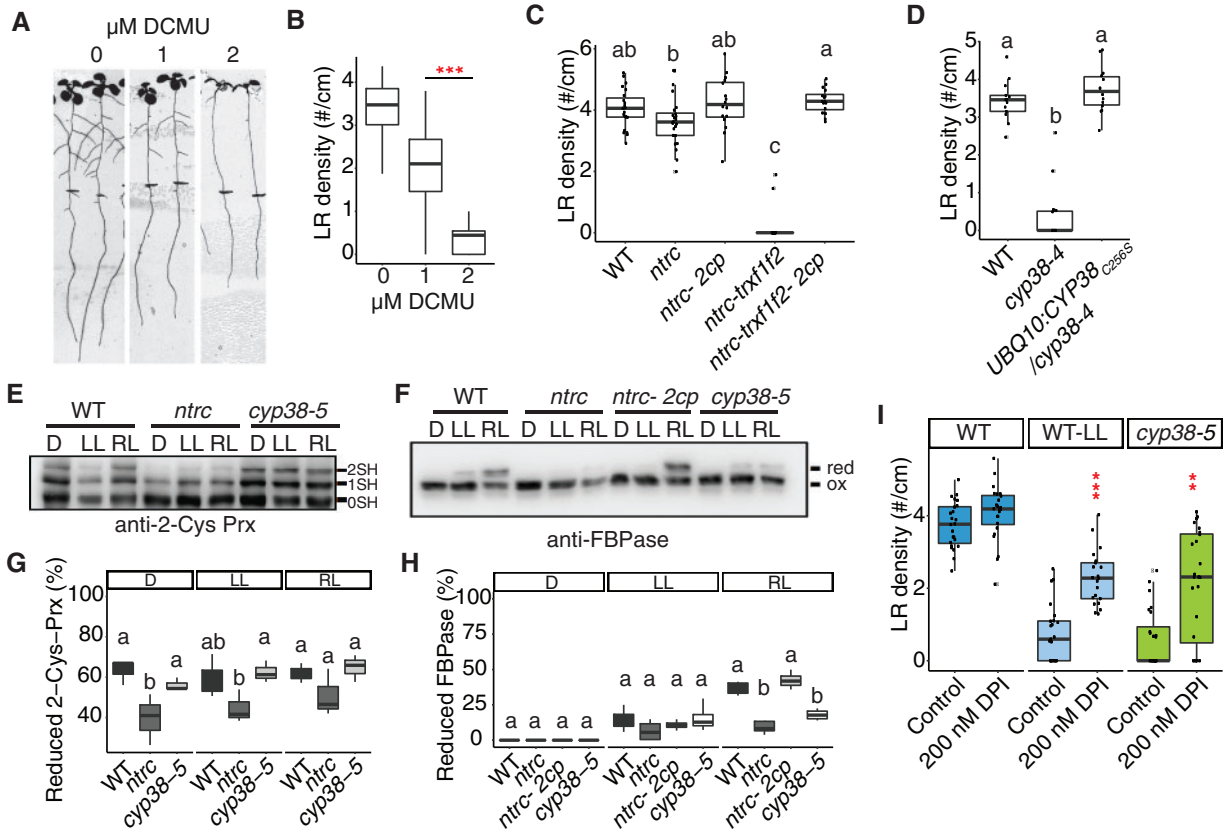

Figure 5 Chloroplast redox status regulates LR emergence. **A**, Scanned images of 10-dpg WT seedlings on 0, 1, and 2 μM DCMU treatment. Root tip positions of 6-dpg are labeled with black marks. The same control panel image is used as in Figure 1H. **B**, Quantification of LR density in WT with and without DCMU treatment (***$P < 0.001$, pairwise *t* test with Hochberg correction, $n > 30$). **C**, Quantifications of LR density in WT, *ntrc*, *ntrc-Δ2cp*, *ntrc-trxf1f2*, and *ntrc-trxf1f1-Δ2cp* mutants under standard growth conditions. Significantly different groups are indicated with letters ($P < 0.05$, pairwise *t* test with Hochberg correction, $n > 16$). **D**, Quantification of LR density in WT, *cyp38-4*, and complemented lines with cysteine to serine mutation in *CYP38* coding sequence. Significantly different groups are indicated with letters ($P < 0.05$, pairwise *t* test with Hochberg correction, $n > 13$ individual T1 complemented lines). **E** and **F,** WT and mutant plants, as indicated, were grown under long-day conditions for 4 weeks at a light intensity of 125 μE m^{-2} s^{-1}. In vivo redox status of 2-Cys Prx (**E**) and FBPase (**F**) proteins was determined at the end of the dark period (**D**) and after 30 min of illumination at 50 μE m^{-2} s^{-1} (LL) or 175 μE m^{-2} s^{-1} (RL). 0SH, 1SH, and 2SH indicate the reduction of zero, one, or two cysteine residues, respectively, of 2-Cys Prx (**E**). Red indicates reduced state and ox marks the oxidized state of FBPase (**F**). **G**, **H**, Quantifications of the proportion of reduced protein from (**E**) and (**F**). Significantly different groups are indicated with letters ($P < 0.05$, pairwise *t* test with Hochberg correction, $n \geq 3$). **I**, Quantifications of LR density in WT, *cyp38-5* under standard light conditions (140 μE m^{-2} s^{-1}) and WT under low light (25 μE m^{-2} s^{-1}), with or without 200 nM DPI treatment (**$P < 0.01$, ***$P < 0.001$, two-way Analysis of variance (ANOVA) comparing WT under control and DPI treatment, $n > 21$).

in *ntrc*, a strong inhibition was observed in *ntrc-trxf1f2* triple mutants (Figure 5C and Supplemental Figure S4B). This strong defect was completely rescued by the *ntrc-Δ2cp* and *ntrc-trxf1f2-Δ2cp* mutants, which lack 2-Cys Prx B and contains a small amount of 2-Cys Prx A in *ntrc* or *ntrc-trxf1f2* background, in line with previous results showing that decreased levels of 2-Cys Prxs restore chloroplast redox homeostasis of NTRC-deficient mutants (Pérez-Ruiz et al., 2017).

Chloroplast cyclophilins have been identified as binding partners of Trx (Motohashi et al., 2003). As reported by Vasudevan et al. (Vasudevan et al., 2012), the mature CYP38 protein contains a single cysteine at position 256 in the cyclophilin domain. We checked whether this cysteine could mediate protein dimerization, through a disulfide bridge, by visualizing the protein on a nonreducing sodium dodecyl sulfate–polyacrylamide gel electrophoresis (SDS–PAGE) gel. However, no apparent dimerization band was found (Supplemental Figure S4C). We also mutated this cysteine to serine and transformed the mutated coding sequence back into *cyp38-4*. Full rescue of the mutant phenotype was observed (Figure 5D), indicating that the function of CYP38 is not dependent on the cysteine and the protein is unlikely to be redox regulated. Because CYP38 has been identified as a potential partner of 2-Cys Prxs (Cerveau et al., 2016), we determined whether this cyclophilin acts as an upstream regulator of these peroxidases. Thus, we evaluated the redox status of 2-Cys Prxs and fructose bisphosphatase (FBPase), included here as a well-established target of the Trx pathway, in mutant plants lacking CYP38. While no difference was observed for 2-Cys Prxs (Figure 5, E and G), light-dependent FBPase reduction was similarly impaired in *cyp38*

and *ntrc* mutants under regular light intensity (Figure 5, F and H). These data indicate that the redox status of some chloroplast proteins may be dependent on CYP38 activity and these proteins may overlap with Trx targets.

We next evaluated photosynthetic performance of CYP38-deficient mutants. Similar to the *ntrc* mutant, here included for comparison, quantum yield of photosystem II (Y(II)) was diminished in *cyp38* plants (Supplemental Figure S4D), indicating that both mutants had similarly affected the efficiency of light energy utilization. Interestingly, energy dissipation through nonphotochemical quenching (Y(NPQ)) was higher in *ntrc* than in the *cyp38* mutants (Supplemental Figure S4E), whereas a substantial elevation of Y(NO), which is an indicator of nonregulated energy dissipation, was only observed in *cyp38* (Supplemental Figure S4F). Overall, these photosynthetic parameters suggest that the *cyp38* mutant does not only have reduced energy conversion efficiency, but is also inefficient in photodamage protection through heat dissipation. These data indicate that potential side reactions, such as excess Reactive Oxygen Species (ROS) production, may occur in *cyp38*, which coincides with previous findings (Wang et al., 2015).

We hypothesized that the reduction in NADPH, rather than the accumulation of ROS, was the major driver of the *cyp38* LR phenotype. This hypothesis is based on the phenotypic similarity of *cyp38* mutants to low-light treated seedlings, which are expected to have decreased ROS levels due to the lower excitation energy being absorbed. Consistent with this hypothesis, adding diphenyleneiodonium chloride (DPI), which inhibits NADPH oxidase activity, partially rescues the LR defect in *cyp38* under standard light conditions, as well as WT root growth under low-light conditions (Figure 5I).

Sucrose, *HY5* and β-cyclocitral-dependent signaling pathways likely regulate LR emergence independently from *CYP38*

Photosynthesis-derived sucrose serves as a long distance signal and resource to promote PR growth (Kircher and Schopfer, 2012). LR development can also be promoted by aerial uptake of sucrose from the media (Macgregor et al., 2008). Consistent with the reduced photosynthetic activity of *cyp38* mutants, we found that early PR growth is highly dependent on supplementary sucrose in the media (Figure 6, A and B). We tested the effects of further increasing sucrose levels by first growing seedlings under our standard conditions (1% sucrose, 140 μE m^{-2} s^{-1} light), then transferring them to the media with additional sucrose (2% and 3%). Further elevating sucrose in the media promoted PR growth in *cyp38-5*, independent of lighting conditions, while WT responded only under low light (Figure 6, C and D). These data suggest that fixed carbon resources may be limiting for PR growth in *cyp38-5* and WT under low-light conditions, and that both genotypes are able to respond when supplementary sucrose is provided in the media. In stark contrast, supplementary sucrose had no significant effect on LR density in *cyp38-5* under standard or low light

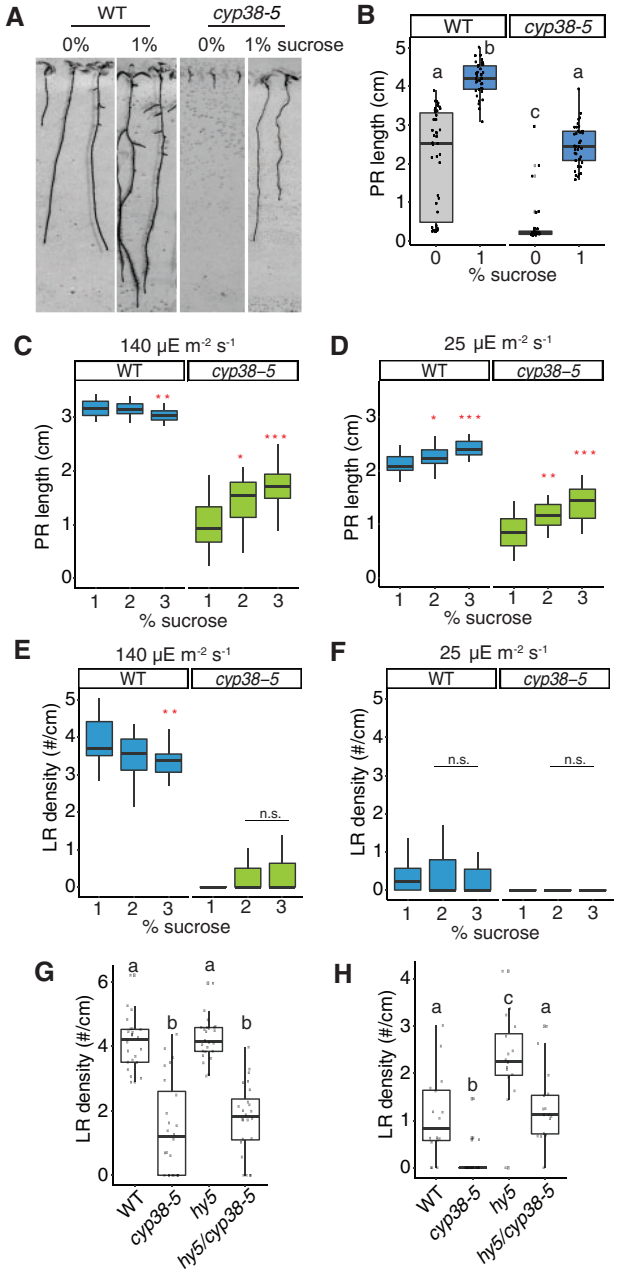

Figure 6 Sucrose and *HY5* signaling are not necessary for *CYP38*-dependent LR emergence. **A**, Scanned images of 9-d-old WT and *cyp38-5* seedlings on 0 and 1% sucrose medium. **B**, Quantifications of PR length comparing WT and *cyp38-5* with 1% or without sucrose. Significantly different groups are indicated with letters ($P < 0.05$, pairwise *t* test with Hochberg correction, $n > 30$). **C** and **D**, Quantifications of PR growth comparing WT and *cyp38-5* under different levels of sucrose in the growth media under regular, 140 μE m^{-2} s^{-1} (**C**) and low light, 25 μE m^{-2} s^{-1} (**D**) conditions (n.s. represents not significant, $^{*}P < 0.05$, $^{**}P < 0.01$, $^{***}P < 0.001$, pairwise *t* test with Hochberg correction $n > 19$). **E** and **F**, Quantifications of LR density comparing WT and *cyp38-5* under different levels of sucrose in the growth media under regular (**E**) and low light (**F**) conditions (n.s. represents not significant, $^{**}P < 0.01$, pairwise *t* test with Hochberg correction, $n > 19$). **G** and **H**, Quantifications of LR density comparing WT, *cyp38-5*, *hy5*, and *hy5/cyp38-5* under regular light (**G**), and low light (**H**) conditions. Significantly different groups are indicated with letters ($P < 0.05$, pairwise *t* test with Hochberg correction, $n > 16$).

conditions, compared to 1% sucrose (Figure 6, E and F). The inability of elevated sucrose to rescue the *cyp38* LR defect is not likely a consequence of prior photo-damage caused by growth under standard light conditions since seedlings grown continuously at 25 μE m^{-2} s^{-1} light were no more responsive to supplementary sucrose (Supplemental Figure S5, A–D). These results suggest that photosynthesis-derived sucrose is essential for PR growth, but is not sufficient to rescue the LR emergence defect in the *cyp38-5* mutant.

HY5 acts as a mobile signal mediating root-to-shoot communication in response to light quantity and quality (Chen et al., 2016; Van Gelderen et al., 2018; Zhang et al., 2019). *hy5* mutants exhibit root systems with reduced PR length; however, LR development is accelerated relative to WT (Zhang et al., 2019). We found that *hy5* mutants showed similar LR density to WT under standard light conditions, while they showed a partial rescue of LR growth under low-light conditions (Figure 6, G and H). These data suggest that *HY5* also mediates light-dependent growth-inhibition of LR development, which confirms a recent study that demonstrated HY5-mediated inhibition of LR development is a local response that occurs in root tissues directly exposed to light (Zhang et al., 2019). To determine whether *HY5* acts in the same genetic pathway as *CYP38*, we compared the phenotypes of *hy5* and *cyp38* single and double mutants. While under standard light conditions the *hy5 cyp38* double mutant had an indistinguishable phenotype from the *cyp38* single mutant; under low-light conditions the double mutant showed an intermediate reduction in LR development between that of *hy5* and *cyp38*, which we interpret as an additive effect (Figure 6, G and H). Together these data suggest that *CYP38* and *HY5* likely regulate root growth through independent pathways, though further investigation is necessary to confirm this genetic interpretation.

Carotenoid biosynthesis affects LR development by mediating pre-branch site formation (Van Norman et al. 2014). Inhibition of carotenoid biosynthesis also results in chloroplast biogenesis defects and therefore may also be indirectly involved in shoot–root communication. Recently, an apoplast carotenoid, β-cyclocitral, has been identified through a chemical screen to be a root growth promoter (Dickinson et al. 2019). We were interested in determining whether β-cyclocitral may act as a *CYP38*-dependent regulator of LRs. Treatment of seedlings with 0.8 μM β-cyclocitral did not cause a significant change in LR emergence under 140 μE m^{-2} s^{-1}; however, we did observe a small but significant increase in LR density in WT under low-light conditions while the *cyp38-5* mutant phenotype was unaffected (Supplemental Figure S5, E and F). Consistent with these findings, we found that the expression levels of carotenoid biosynthesis genes were not affected in *cyp38-5* (Supplemental Figure S5G). Together, these data support a role for β-cyclocitral in a *CYP38*-independent pathway regulating LR growth; however, further investigation is needed to determine whether this carotenoid derivative normally plays a role in mediating root developmental responses to light intensity.

Downregulation of auxin biosynthesis and signaling mediate the *cyp38* phenotype in roots

Shoot-derived auxin has been shown to be important for LR emergence (Reed et al., 1998; Bhalerao et al., 2002; Swarup et al., 2008). However, it is less clear whether the shoot-synthesized auxin is dependent on photosynthesis, other light-dependent processes, or simply on the size of the shoot. First, we investigated whether the LR defect in *cyp38* mutants is mediated by altered activity of the auxin pathway. Measurement of IAA levels in the mutant and WT under varying light intensity showed that IAA accumulates to a higher level in the root than shoot in 10-d-old seedlings, and its abundance in root tissues is significantly reduced in the *cyp38-5* mutant as well as under low-light conditions (Figure 7A). Note that these measurements are normalized to fresh weight and, thus, account for differences in root or shoot system size between genotypes. Using grafted plants, we found that IAA levels were the highest in roots when the genotype of the shoot is WT, compared to plants where the shoot was grafted from *cyp38-5* mutants (Figure 7B). These data suggest either that auxin, or a systemically acting signal that induces auxin biosynthesis, is synthesized in the shoot and transmitted to the root in a light intensity and *CYP38*-dependent manner.

Using a transcriptional reporter of auxin response, *pDR5rev::3XVENUS-N7* (Heisler et al., 2005), we found that reporter activity in the PR tip is similar between WT and *cyp38*, while it is dramatically reduced in more distal mature tissues of *cyp38* (Figure 7C). Auxin accumulates in the cortex cells surrounding LRP and induces expression of cell wall-degrading proteins that facilitate the emergence of LRP (Swarup et al., 2008). We quantified *pDR5rev:3XVENUS-N7* expression in these cortical cells, and observed a significant reduction in the *cyp38* mutant compared to WT (Figure 7, D and E). Low-light treatment also reduced reporter activity in these tissues as early as 8 h (Figure 7, F and G), suggesting that large morphological changes are not needed to induce differences in auxin signaling. Consistent with these observations, exogenous IAA treatment largely rescued LR emergence in both *cyp38-5* and low-light-treated WT seedlings (Figure 7H). The conversion of IPA into IAA is dependent on NADPH-dependent reduction (Cha et al., 2015), and it may be that lower photosynthetic output limits auxin biosynthesis.

Discussion

The differentiated functions of organs in complex multicellular plants require that resources are shared across the body and systemic signals coordinate responses to environmental change. Here, we show that photosynthetic activity in shoots has a systemic effect on root system architecture, likely by affecting the biosynthesis of auxin. In the root system, the systemic signal regulates the rate at which LRs proceed through the emergence stage. LR emergence disrupts the structural integrity of the plant body. Thus, pre-emergence may be an optimal "holding ground" for LRs that are already patterned, but where the plant is not ready to

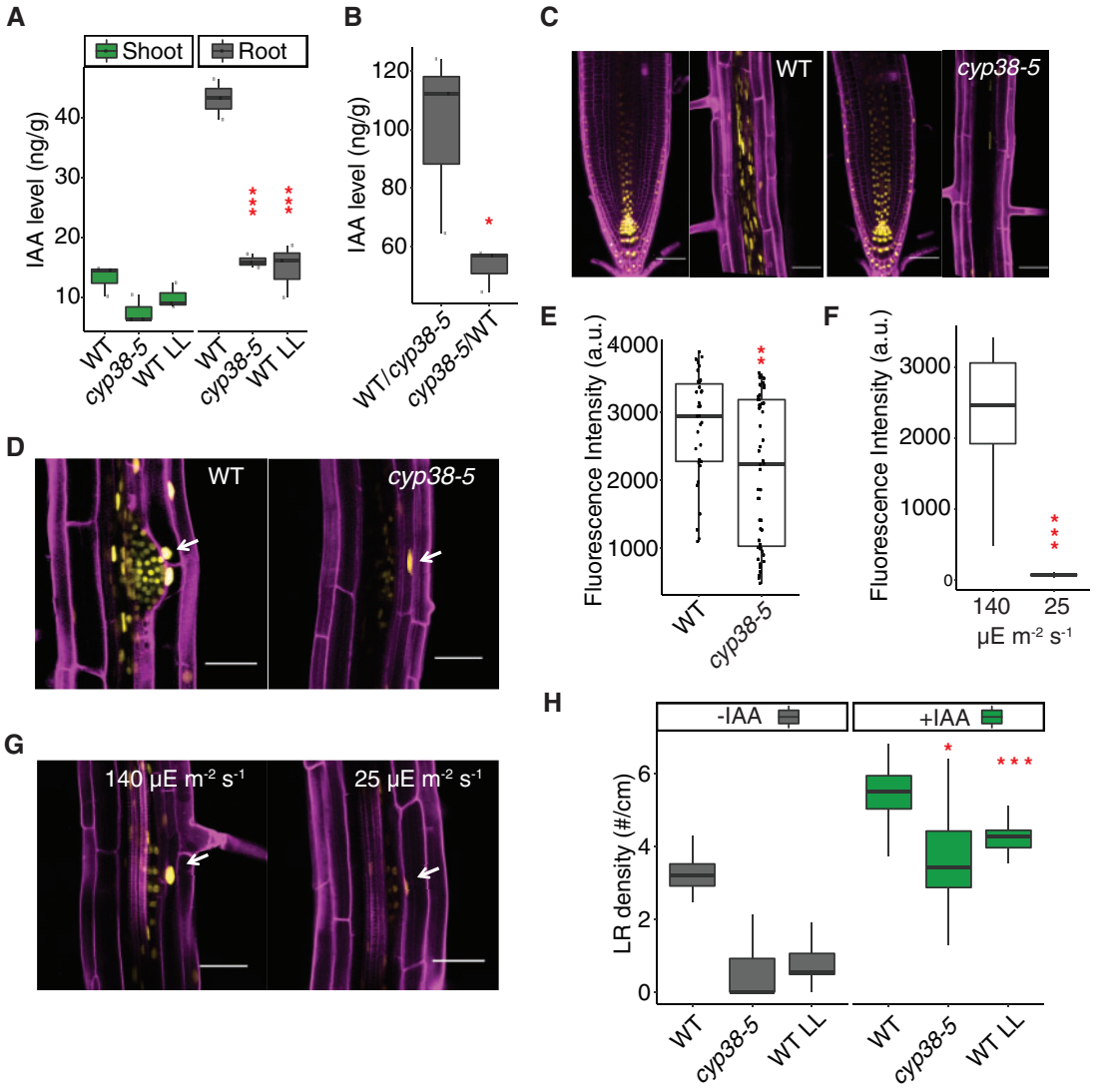

Figure 7 Auxin is involved in *CYP38*-dependent regulation of LRs. **A**, Measurements of IAA levels in WT and *cyp38-5* under standard light and WT under low light in shoot and root tissues. (***$P < 0.001$, pairwise *t* test with Hochberg correction, $n = 3$). **B**, Measurements of IAA level in the rootstock of WT/*cyp38-5* and *cyp38-5*/WT grafted plants. (*$P < 0.05$, pairwise *t* test, $n = 3$). **C**, Confocal images of *pDR5rev::3XVenus-N7* in PR tip and mature region of PR in WT (left panel), or in *cyp38-5* (right panel). Scale bars = 50 μm. **D**, Confocal images of *pDR5rev::3XVenus-N7* in LRP in WT and *cyp38-5*. Arrows point to expression in the cortex tissue layer surrounding a LRP. Scale bars = 50 µm. **E**, Measurements of the fluorescence intensity of *pDR5rev::3XVenus-N7* in cortex cells surrounding LRP in WT and *cyp38-5* (**$P < 0.01$, pairwise *t* test, $n > 36$). **F**, Measurements of the fluorescence intensity of *pDR5rev::3XVenus-N7* in cortex cells surrounding LRP in WT under both regular light (140 µE m^{-2} s^{-1}) and 8 h of low light (25 µE m^{-2} s^{-1}) treatment (**$P < 0.01$, pairwise *t* test, $n > 30$). **G**, Confocal images of *pDR5rev::3XVenus-N7* in LRP in WT under regular light (140 µE m^{-2} s^{-1}) and 8 h of low light (25 µE m^{-2} s^{-1}) treatment. Arrows point to the expression in the cortex tissue layer surrounding a LRP. Scale bars = 50 µm. **H**, Quantification of LR density in WT and *cyp38* mutant with or without 1 µM IAA treatment (*$P < 0.05$, ***$P < 0.001$, two-way ANOVA comparing with WT under control or IAA treatment, $n > 20$).

make a full investment in post-emergence growth. In this way the root system maintains developmental flexibility, potentially enabling the plant to exploit shifts in the environment when light intensity increases.

While the approaches we have used to tune photosynthetic activity were varied and included genetic, environmental, nutritional, and pharmacological perturbations, it is a challenge to alter this central metabolic pathway without causing many indirect effects on the physiology of the plant. Indeed, Fu et al. demonstrated that necrosis and severe growth defects arise in the *cyp38* mutant when light intensity reaches 300 µmol m^{-2} s^{-1} (Fu et al., 2007). Furthermore, *cyp38* seedling viability under in vitro conditions is dependent on supplementary sucrose (Figure 6A).

We propose three hypotheses to explain the reduction in LR development in *cyp38* mutants. Our first hypothesis is that the physiological stress caused by PSII instability leads to the inhibition of LR growth. This hypothesis is unlikely, as treatment of WT seedlings with a period of reduced light intensity causes a similar reduction in auxin signaling and LR

emergence as the *cyp38* mutant (Figure 4 and Figure 7, G and H). Furthermore, the *cyp38* phenotype is enhanced, not suppressed, under low-light conditions (Figure 6, E and F). Our second hypothesis is that *cyp38* mutants and low-light conditions cause a reduction in LR development due to their smaller shoot size, which affects the amount of auxin transmitted between the shoot and root. This hypothesis is difficult to test directly since photosynthetic output will be directly related to shoot growth. That said, several lines of evidence are inconsistent with this hypothesis. If shoot size differences explain the changes in root development, then these differences should accumulate slowly over time, as the difference in shoot size accumulates over the life of the seedling. In contrast, the effects of reduced light intensity are translated rapidly into a large difference in auxin signaling 8 h after treatment (Figure 7, F and G) and, for LR emergence, just one day after treatment (Figure 4, D and E). Furthermore, if LR growth simply corresponds with shoot size, the allometric relationship between seedling developmental stage and LR growth would not differ as it does between WT and *cyp38* mutants (Figure 1K). Perhaps most convincing is that *cyp38* seedlings, analyzed later in their development, have far fewer LRs than expected, particularly in comparison to younger WT seedlings with smaller shoots (Figure 1, H–J). These data strongly favor a third hypothesis, that differences in photosynthetic activity, rather than physiological stress or differences in shoot size, are the primary driver of the LR phenotypes observed in *cyp38* and low-light conditions.

A key signal that relays photosynthetic activity from shoots to roots is likely auxin. Auxin levels spike at 5–7 d after germination in Arabidopsis seedlings and are derived from the first true leaves that emerge at this stage (Bhalerao et al., 2002). Excising of the seedling shoot inhibits LR emergence, while conversion of the inactive IAM to IAA, using shoot-specific expression of IAAH, rescues LR emergence (Swarup et al., 2008). Our work has revealed a connection between photosynthesis and auxin synthesis, supported by the observed reduction in auxin levels in the root of *cyp38*, as well as in roots grown under reduced light intensity (Figure 7). Consistently, supplementing *cyp38* mutants with IAA rescues the LR emergence phenotype. While auxin transport was not directly measured in this study, the shoot-specific necessity for *CYP38* function strongly argues that auxin, or a transportable auxin precursor, is synthesized in the shoot and becomes limiting for LR growth when photosynthetic activity is lowered.

As a result of lower photosynthetic activity, NADPH production should fall. NADPH acts as the major electron donor for various metabolic reactions and redox-regulated proteins in the chloroplast. Disruption of NTRC function, a well characterized reductase that uses NADPH to reduce downstream proteins, results in defects in LR development similar to *cyp38*, particularly when combined with mutations in two of its target Trxs (Kirchsteiger et al., 2012). These genetic results highlight the importance of chloroplast redox capacity in supporting root architecture, which suggests two potential models for CYP38 protein function. First, CYP38 may accept electrons directly from the NTRC-trx pathway via membrane localized Trx-like proteins and reduce downstream proteins. This hypothesis is supported by the direct interaction observed between CYP38 and Trx and the role of a related cyclophilin protein, CYP20, in reducing a metabolic enzyme in the chloroplast (Motohashi et al., 2003; Park et al., 2013). Alternatively, CYP38 may not be a direct target of NTRC-trx, but its function in PSII assembly and maintenance ensures efficient electron flow, thus indirectly affecting NADPH production and associated downstream redox reactions. Although FBPase shows CYP38-dependent redox states (Figure 5, F and H), the cysteine residue in CYP38 does not play any obvious role in protein function (Figure 5D). Thus, our results support a function for CYP38 specifically in promoting PSII-specific functions, but cannot rule out more specific functions in regulating cellular redox through physical association with redox pathway components.

How do these chloroplast-specific processes affect auxin biosynthesis? The chloroplast also serves as a major site for the biosynthesis of various plant hormones (Lu and Yao, 2018). For example, tryptophan, the precursor of auxin, is synthesized in the chloroplast (Radwanski and Last, 1995), and then converted to IAA through YUCCA (YUC) flavin monooxygenase-like proteins, through an NADPH and oxygen-dependent reaction (Zhao, 2012). Interestingly, YUC6 has been found to possess Trx activity (Cha et al., 2015), which is directly regulated by an NADPH-dependent Trx reductase. We have found that the treatment of seedlings with NADPH oxidase inhibitors, which are expected to cause an accumulation of NADPH, partially rescues LR emergence in *cyp38* and WT under low-light conditions (Figure 5I). Thus, the current model we propose is that changes in photosynthetic activity directly modulate auxin levels through the redox capacity of the chloroplast and the rate of redox-dependent biosynthetic reactions.

Conclusions

In summary, our work has characterized an important function for photosynthetic activity in the regulation of root system architecture, through the detailed characterization of *CYP38* function. We have shown that a specific stage of LR development is regulated through systemic signals derived from the shoot. Our findings indicated that this systemic regulation is independent of sucrose, HY5, or β-cyclocitral, which are known long-distance signals for root system regulation. Instead, we suggest that auxin biosynthesis is linked to cellular redox state and that this hormone transmits the long-distance signal to regulate LR emergence.

Materials and methods

Plant materials

The *cyp38-4* mutant allele was derived from an EMS mutagenized population of *Arabidopsis thaliana*, Col-0. The *cyp38-5* allele was obtained from ABRC with the stock

number SALK_029448. The *hy5* mutant was obtained from ABRC with the stock number SALK_096651. The *ntrc*, *ntrc-Δ2cp*, *ntrc-trxf1f2*, and *ntrc-trxf1f2-Δ2cp* lines are previously described (Pérez-Ruiz et al., 2017). Auxin reporter, *pDR5rev::3XVENUS-N7* was previously described (Heisler et al., 2005). *Arabidopsis thaliana* ecotype Columbia (Col-0) was used as the reference strain throughout the entire study.

Plant growth conditions

Sterilized seeds were grown on sterile 0.7% Gelzan media containing 1X Murashige and Skoog nutrients (MSP01-50LT, Caisson) and 1% sucrose. Seedlings were grown under standard light intensity (140 μE m^{-2} s^{-1}) for 5–6 d before transfer to standard media supplemented with chemicals, or reduced light conditions for 3–5 d. The position of the root tip was marked at the time of transfer. Supplements include IAA, DCMU, and DPI (Sigma-Aldrich). Growth of seedlings was performed in a Percival CU41L4 incubator at a constant temperature of 22°C with long-day lighting conditions (16 h light and 8 h dark). Plates were sealed with both parafilm and micropore tape (3M) as previously described (Duan et al., 2013).

Transgene construction

Golden gate cloning was used to assemble various DNA fragments into pSE7 vector (Emami et al., 2013). The *proCYP38:CYP38* construct was generated by cloning a 5.1-kb genomic CYP38 fragment into Zero Blunt TOPO vector with the primers listed in Supplemental Table S1. A 3-kb promoter region was used to generate the *proCYP38:erGFP* reporter construct. A VENUS-derived fluorescence protein, Ypet (Song et al., 2016), 2.5-kb *UBQ10* promoter, and *CYP38* coding sequence were used to assemble *proUBQ10:CYP38-Ypet*. Site-directed mutagenesis was used to introduce the Cys to Ser mutation into the *CYP38* coding sequence in order to generate *proUBQ10:CYP38_c256s*. All primers used for cloning are listed in Supplemental Table S1. Transgenic plants were generated by a standard floral dip method into the *cyp38-4* background. Seeds were harvested from transformed plants and selected visually based on mCherry fluorescence using an M165 FC fluorescence microscope (Leica) under a DsRed filter (512/630 nm).

Microscopic analysis

For quantitation of LR developmental stages, roots were mounted in a modified Hoyer solution (chloral hydrate:water:glycerol in proportions 8:2:1, g/mL/mL), then imaged using a Leica DMI6000 inverted compound microscope with 20× objective. For confocal microscopy, roots were mounted in 5 μg/mL propidium iodide (PI) solution (Thermal Fisher), and imaged using a Leica SP8 point-scanning confocal microscope, with a 20× objective. The 488-nm laser was used to detect green fluorescent protein (GFP) and PI staining, and 512-nm laser was used for Ypet fluorescence excitation. Image processing and fluorescence quantification were all performed using ImageJ software.

Grafting and root phenotypic analysis

For nongrafted plants, the emerged LRs were captured using a Epson dual light scanner v800 with 8- to 11-dpg seedlings. LR density and PR length were quantified using ImageJ. For grafting experiments, a transverse cut was made at the upper part of the hypocotyl of 5-dpg seedlings, and combinations between WT and *cyp38-5* scions and root stocks were assembled by attaching the transverse cut surfaces together (Melnyk, 2017). These recombined seedlings were then left on wet filter paper plus Hybond N membrane for 5 d in a growth chamber to allow the formation of the junction. Any shoot-borne roots were removed during that process. After that, the seedlings were transferred back to standard medium for recovery. Scanned root images were taken 7 d after recovery for the quantification of total root branches.

Protoplast transformation

To better visualize the cellular localization of CYP38 protein, protoplasts were isolated from 3- to 4-week-old Arabidopsis Col-0 plant rosette leaves, and the *proUBQ10:CYP38-Ypet* construct was transformed into the protoplasts using the Poly Ethylene Glycol-calcium method (Yoo et al., 2007). The transformed protoplasts were then imaged using an SP8 confocal microscope.

Plant hormones measurements

For plant hormone measurements, 10-d-old WT and *cyp38-5* seedlings grown under standard light conditions and WT grown under low-light conditions were used. For IAA measurements in grafted plants, 20-d-old WT/*cyp38-5* and *cyp38-5*/WT grown under regular light conditions were used. More than 100 mg of the sample was weighed out and, after vortexing and pipetting in and out several times to make sure the solution was homogeneous, was dried down in a 2-mL Eppendorf tube. Hormones were extracted using cold methanol: acetonitrile (50:50, v/v) spiked with deuterium-labeled internal standards (1.25 μM of IAA-D5). The sample was shaken for 25 min and centrifuged at 16,000*g* for 10 min. The supernatant was transferred to a new tube and the extraction of the pellet was repeated one more time. The supernatants were pooled and dried down using a speed-vac. The pellets were re-dissolved in 200 μL of 15% methanol. For LC separation, a ZORBAX Eclipse Plus C18 column (2.1 mm × 100 mm, Agilent) was used flowing at 0.45 mL/min. The gradient of the mobile phases A (0.1% formic acid) and B (0.1% formic acid/90% acetonitrile) was as follows: 5% B for 1 min, to 60% B in 4 min, to 100% B in 2 min, hold at 100% B for 3 min, to 5% B in 0.5 min. The Shimadzu LC system was interfaced with a Sciex QTRAP 6500 + mass spectrometer equipped with a TurboIonSpray electrospray ion source. Analyst software (version 1.6.3) was used to control sample acquisition and data analysis. The QTRAP 6500 + mass spectrometer was tuned and calibrated according to the manufacturer's recommendations. The hormones were detected using Multiple Reaction Monitoring transitions that were optimized using standards. The instrument was set-up to acquire in both positive and negative ion

switching. For quantification, an external standard curve was prepared using a series of standard samples containing different concentrations of unlabeled hormones and fixed concentrations of the deuterium-labeled standards mixture.

The data were normalized based on the internal standards: IAA-D5, to account for experimental variation and hormone extraction/ionization efficiency. The amounts in ng/g of the hormones detected are reported. Sample loading and data extraction were performed by Creative Proteomics Service (45-1 Ramsey Road, Shirley, NY 11967, USA).

Western blot analysis

Plant tissues were ground in liquid nitrogen to a fine powder. Alkylation assays were performed as previously described (Pérez-Ruiz et al., 2017) using 10 mM methyl-maleimide polyethylene glycol (2-Cys Prx) or 60 mM iodoacetamide (FBPase and CYP38). Protein samples were subjected to reducing (2-Cys Prx) or nonreducing (CYP38 and FBPase) SDS–PAGE using acrylamide gel concentration of 9.5% (FBPase and CYP38) and 14% (2-Cys Prx). Resolved proteins were transferred to nitrocellulose membranes and probed with the indicated antibodies. Specific antibody for 2-Cys Prx was previously raised (Pérez-Ruiz et al., 2006). The anti-FBPase antibody was kindly provided by Dr Sahrawy (Estación Experimental del Zaidín, Granada, Spain). Antibody for CYP38 was purchased from Agrisera (Sweden).

Measurements of photosynthetic parameters

Measurement of chlorophyll *a* fluorescence at room temperature was performed using a pulse-amplitude modulation fluorometer (IMAGING-PAM M-Series instrument, Walz, Effeltrich, Germany). Induction–recovery curves were performed using blue (450 nm) actinic light (81 μE m^{-2} s^{-1}) at the intensities specified for each experiment during 6 min. Saturating pulses of blue light (10,000 μE m^{-2} s^{-1}) and 0.6-s duration were applied every 60 s, and recovery in darkness was recorded for another 6 min. The parameters Y(II), Y(NPQ), and Y(NO) corresponding to the respective quantum yields of PSII photochemistry, nonregulated basal quenching, and nonregulated energy dissipation, were calculated by the ImagingWin v2.46i software according to the equations described in Kramer et al. (2004).

Data plotting and statistics

For all the boxplots, the various elements are defined as follows: upper whisker = largest observation less than or equal to upper hinge + 1.5 * interquartile range (IQR); lower whisker = smallest observation greater than or equal to lower hinge − 1.5 * IQR; center line = median, 50% quantile; upper hinge = 75% quantile; lower hinge = 25% quantile; outliers = > 1.5 * IQR beyond either end of the box; each dot in the box represents a single data points.

Pairwise *t* test with Hochberg correction or two-way ANOVA were performed based on the different needs of data interpretation.

Accession numbers

The sequence data for the following Arabidopsis genes can be found in the Arabidopsis Information Resource database (https//www.arabidopsis.org): AT3G01480 (*CYP38*), AT2G41680 (*NTRC*), AT3G02730 (*TRXF1*), AT5G16400 (*TRXF2*), AT3G11630 (*2-CYS PRX A*), AT5G06290 (*2-CYS PRX B*), AT3G54050 (*FBPase*), and AT5G11260 (*HY5*).

Supplemental data

The following materials are available in the online version of this article.

Supplemental Figure S1. Mapping output of *cyp38-4*.

Supplemental Figure S2. CYP38-Ypet fusion protein promotes root branching from the shoot.

Supplemental Figure S3. The quantity of light is perceived by the shoot to affect LRs.

Supplemental Figure S4. CYP38-dependent root phenotype is derived from photosynthetic status in the shoot.

Supplemental Figure S5. Sucrose and β-cyclocitral likely regulate LR development in a CYP38-independent manner.

Acknowledgments

We thank the members of Dinneny lab for their discussions during the preparation of this manuscript.

Funding

The funding was provided by Carnegie Institution for Science Endowment to J.R.D., and European Regional Development Fund-co-financed grant (BIO2017-85195-C2-1-P) from the Spanish Ministry of Economy, Industry and Competitiveness to F.J.C. The plant hormone measurements were provided by Creative Proteomics. The research of J.R.D. was supported in part by a Faculty Scholar grant from the Howard Hughes Medical Institute and the Simons Foundation.

Conflict of interest statement. None declared.

References

Bhalerao RP, Eklöf J, Ljung K, Marchant A, Bennett M, Sandberg G (2002) Shoot-derived auxin is essential for early lateral root emergence in Arabidopsis seedlings. Plant J **29**: 325–332

Bloom A (2005) Coordination between shoots and roots. In NM Holbrook, MA Zwieniecki, eds, Vascular Transport in Plants. Academic Press, Burlington, pp. 241–256

Cerveau D, Kraut A, Stotz HU, Mueller MJ, Couté Y, Rey P (2016) Characterization of the Arabidopsis thaliana 2-Cys peroxiredoxin interactome. Plant Sci **252**: 30–41

Cha J-Y, Kim W-Y, Kang SB, Kim JI, Baek D, Jung IJ, Kim MR, Li N, Kim H-J, Nakajima M, et al. (2015) A novel thiol-reductase activity of Arabidopsis YUC6 confers drought tolerance independently of auxin biosynthesis. Nat Commun **6**: 8041

Chang T-G, Zhu X-G, Raines C (2017) Source-sink interaction: a century old concept under the light of modern molecular systems biology. J Exp Bot **68**: 4417–4431

Chen X, Yao Q, Gao X, Jiang C, Harberd NP, Fu X (2016) Shoot-to-root mobile transcription factor HY5 coordinates plant carbon and nitrogen acquisition. Curr Biol **26**: 640–646

Dickinson AJ, Lehner K, Mi J, Jia K-P, Mijar M, Dinneny J, Al-Babili S, Benfey PN (2019) β-Cyclocitral is a conserved root growth regulator. Proc Natl Acad Sci USA **116**: 10563–10567

de Wit M, Galvão VC, Fankhauser C (2016) Light-mediated hormonal regulation of plant growth and development. Annu Rev Plant Biol **67**: 513–537

Duan L, Dietrich D, Ng CH, Chan PMY, Bhalerao R, Bennett MJ, Dinneny JR (2013) Endodermal ABA signaling promotes lateral root quiescence during salt stress in Arabidopsis seedlings. Plant Cell **25**: 324–341

Emami S, Yee M-C, Dinneny JR (2013) A robust family of Golden Gate Agrobacterium vectors for plant synthetic biology. Front Plant Sci **4**: 339

Fernández-Marcos M, Desvoyes B, Manzano C, Liberman LM, Benfey PN, Del Pozo JC, Gutierrez C (2017) Control of Arabidopsis lateral root primordium boundaries by MYB36. New Phytol **213**: 105–112

Fu A, He Z, Cho HS, Lima A, Buchanan BB, Luan S (2007) A chloroplast cyclophilin functions in the assembly and maintenance of photosystem II in Arabidopsis thaliana. Proc Natl Acad Sci USA **104**: 15947–15952

Halliday KJ, Martínez-García JF, Josse E-M (2009) Integration of light and auxin signaling. Cold Spring Harb Perspect Biol **1**: a001586

Heisler MG, Ohno C, Das P, Sieber P, Reddy GV, Long JA, Meyerowitz EM (2005) Patterns of auxin transport and gene expression during primordium development revealed by live imaging of the Arabidopsis inflorescence meristem. Curr Biol **15**: 1899–1911

Hersch M, Lorrain S, de Wit M, Trevisan M, Ljung K, Bergmann S, Fankhauser C (2014) Light intensity modulates the regulatory network of the shade avoidance response in Arabidopsis. Proc Natl Acad Sci USA **111**: 6515–6520

Ivanchenko MG, Zhu J, Wang B, Medvecká E, Du Y, Azzarello E, Mancuso S, Megraw M, Filichkin S, Dubrovsky JG, et al. (2015) The cyclophilin A DIAGEOTROPICA gene affects auxin transport in both root and shoot to control lateral root formation. Development **142**: 712–721

Kerk NM, Feldman NJ (1995) A biochemical model for the initiation and maintenance of the quiescent center: implications for organization of root meristems. Development **121**: 2825–2833

Kircher S, Schopfer P (2012) Photosynthetic sucrose acts as cotyledon-derived long-distance signal to control root growth during early seedling development in Arabidopsis. Proc Natl Acad Sci USA **109**: 11217–11221

Kirchsteiger K, Ferrández J, Pascual MB, González M, Cejudo FJ (2012) NADPH thioredoxin reductase C is localized in plastids of photosynthetic and nonphotosynthetic tissues and is involved in lateral root formation in Arabidopsis. Plant Cell **24**: 1534–1548

Kramer DM, Johnson G, Kiirats O, Edwards GE (2004) New fluorescence parameters for the determination of QA redox state and excitation energy fluxes. Photosynth Res **79**: 209

Laskowski MJ, Williams ME, Nusbaum HC, Sussex IM (1995) Formation of lateral root meristems is a two-stage process. Development **121**: 3303–3310

Lucas M, Kenobi K, von Wangenheim D, Voβ U, Swarup K, De Smet I, Van Damme D, Lawrence T, Péret B, Moscardi E, et al. (2013) Lateral root morphogenesis is dependent on the mechanical properties of the overlaying tissues. Proc Natl Acad Sci USA **110**: 5229–5234

Lu Y, Yao J (2018) Chloroplasts at the crossroad of photosynthesis, pathogen infection and plant defense. Int J Mol Sci **19**: 3900

Macgregor DR, Deak KI, Ingram PA, Malamy JE (2008) Root system architecture in Arabidopsis grown in culture is regulated by sucrose uptake in the aerial tissues. Plant Cell **20**: 2643–2660

Malamy JE, Benfey PN (1997) Organization and cell differentiation in lateral roots of Arabidopsis thaliana. Development **124**: 33–44

Mashiguchi K, Tanaka K, Sakai T, Sugawara S, Kawaide H, Natsume M, Hanada A, Yaeno T, Shirasu K, Yao H, et al. (2011) The main auxin biosynthesis pathway in Arabidopsis. Proc Natl Acad Sci USA **108**: 18512–18517

McDavid CR, Sagar GR, Marshall C (1972) The effect of auxin from the shoot on root development in Pisum sativum L. New Phytol **71**: 1027–1032

Melnyk CW (2017) Grafting with Arabidopsis thaliana. Methods Mol Biol **1497**: 9–18

Moreno-Risueno MA, Van Norman JM, Moreno A, Zhang J, Ahnert SE, Benfey PN (2010) Oscillating gene expression determines competence for periodic Arabidopsis root branching. Science **329**: 1306–1311

Motohashi K, Koyama F, Nakanishi Y, Ueoka-Nakanishi H, Hisabori T (2003) Chloroplast cyclophilin is a target protein of thioredoxin. Thiol modulation of the peptidyl-prolyl cis-trans isomerase activity. J Biol Chem **278**: 31848–31852

Orman-Ligeza B, Parizot B, de Rycke R, Fernandez A, Himschoot E, Van Breusegem F, Bennett MJ, Périlleux C, Beeckman T, Draye X (2016) RBOH-mediated ROS production facilitates lateral root emergence in Arabidopsis. Development **143**: 3328–3339

Park S-W, Li W, Viehhauser A, He B, Kim S, Nilsson AK, Andersson MX, Kittle JD, Ambavaram MMR, Luan S, et al. (2013) Cyclophilin 20-3 relays a 12-oxo-phytodienoic acid signal during stress responsive regulation of cellular redox homeostasis. Proc Natl Acad Sci USA **110**: 9559–9564

Péret B, Li G, Zhao J, Band LR, Voß U, Postaire O, Luu D-T, Da Ines O, Casimiro I, Lucas M, et al. (2012) Auxin regulates aquaporin function to facilitate lateral root emergence. Nat Cell Biol **14**: 991–998

Pérez-Ruiz JM, Naranjo B, Ojeda V, Guinea M, Cejudo FJ (2017) NTRC-dependent redox balance of 2-Cys peroxiredoxins is needed for optimal function of the photosynthetic apparatus. Proc Natl Acad Sci USA **114**: 12069–12074

Pérez-Ruiz JM, Spínola MC, Kirchsteiger K, Moreno J, Sahrawy M, Cejudo FJ (2006) Rice NTRC is a high-efficiency redox system for chloroplast protection against oxidative damage. Plant Cell **18**: 2356–2368

Puig J, Pauluzzi G, Guiderdoni E, Gantet P (2012) Regulation of shoot and root development through mutual signaling. Mol Plant **5**: 974–983

Radwanski ER, Last RL (1995) Tryptophan biosynthesis and metabolism: biochemical and molecular genetics. Plant Cell **7**: 921–934

Reed RC, Brady SR, Muday GK (1998) Inhibition of auxin movement from the shoot into the root inhibits lateral root development in Arabidopsis. Plant Physiol **118**: 1369–1378

Rellán-Álvarez R, Lobet G, Lindner H, Pradier P-L, Sebastian J, Yee M-C, Geng Y, Trontin C, LaRue T, Schrager-Lavelle A, et al. (2015) GLO-Roots: an imaging platform enabling multidimensional characterization of soil-grown root systems. eLife **4**: e07597.

Rost TL (1986) The control of lateral root development in cultured pea seedlings. I. The role of seedling organs and plant growth regulators. Bot Gaz **147**: 137–147

Rowntree RA, Morris DA (1979) Accumulation of 14C from exogenous labelled auxin in lateral root primordia of intact pea seedlings (Pisum sativum L.). Planta **144**: 463–466

Serrato AJ, Pérez-Ruiz JM, Spínola MC, Cejudo FJ (2004) A novel NADPH thioredoxin reductase, localized in the chloroplast, which deficiency causes hypersensitivity to abiotic stress in Arabidopsis thaliana. J Biol Chem **279**: 43821–43827

Sirpiög S, Khrouchtchova A, Allahverdiyeva Y, Hansson M, Fristedt R, Vener AV, Scheller HV, Jensen PE, Haldrup A, Aro E-M (2008) AtCYP38 ensures early biogenesis, correct assembly and sustenance of photosystem II. Plant J **55**: 639–651

Song L, Huang S-SC, Wise A, Castanon R, Nery JR, Chen H, Watanabe M, Thomas J, Bar-Joseph Z, Ecker JR (2016) A transcription factor hierarchy defines an environmental stress response network. Science **354**: aag1550

Spiegelman Z, Ham B-K, Zhang Z, Toal TW, Brady SM, Zheng Y, Fei Z, Lucas WJ, Wolf S (2015) A tomato phloem-mobile protein regulates the shoot-to-root ratio by mediating the auxin response in distant organs. Plant J **83**: 853–863

Swarup K, Benkova E, Swarup R, Casimiro I, Peret B, Yang Y, Parry G, Nielsen E, De Smet I, Vanneste S, et al. (2008) The auxin influx carrier LAX3 promotes lateral root emergence. Nat Cell Biol **10**: 946–954

Van Gelderen K, Kang C, Paalman R, Keuskamp D, Hayes S, Pierik R (2018) Far-red light detection in the shoot regulates lateral root development through the HY5 transcription factor. Plant Cell **30**: 101–116

Van Norman JM, Xuan W, Beeckman T, Benfey PN (2013) To branch or not to branch: the role of pre-patterning in lateral root formation. Development **140**: 4301–4310

Van Norman JM, Zhang J, Cazzonelli CI, Pogson BJ, Harrison PJ, Bugg TDH, Chan KX, Thompson AJ, Benfey PN (2014) Periodic root branching in Arabidopsis requires synthesis of an uncharacterized carotenoid derivative. Proc Natl Acad Sci USA **111**: E1300–E1309

Vasudevan D, Fu A, Luan S, Swaminathan K (2012) Crystal structure of Arabidopsis cyclophilin38 reveals a previously uncharacterized immunophilin fold and a possible autoinhibitory mechanism. Plant Cell **24**: 2666–2674

Vermeer JEM, von Wangenheim D, Barberon M, Lee Y, Stelzer EHK, Maizel A, Geldner N (2014) A spatial accommodation by neighboring cells is required for organ initiation in Arabidopsis. Science **343**: 178–183

Wang Y, Zeng L, Xing D (2015) ROS-mediated enhanced transcription of CYP38 promotes the plant tolerance to high light stress by suppressing GTPase activation of PsbO2. Front Plant Sci **6**: 777

Wightman F, Thimann KV (1980) Hormonal factors controlling the initiation and development of lateral roots: I. Sources of primordia-inducing substances in the primary root of pea seedlings. Physiol Plant **49**: 13–20

Yoo S-D, Cho Y-H, Sheen J (2007) Arabidopsis mesophyll protoplasts: a versatile cell system for transient gene expression analysis. Nature Protocols **2**: 1565–1572

Zhang Y, Wang C, Xu H, Shi X, Zhen W, Hu Z, Huang J, Zheng Y, Huang P, Zhang K-X, et al. (2019) HY5 contributes to light-regulated root system architecture under a root-covered culture system. Front Plant Sci **10**: 1490

Zhao Y (2012) Auxin biosynthesis: a simple two-step pathway converts tryptophan to indole-3-acetic acid in plants. Mol Plant **5**: 334–338